

# Mass Spectrometric Study of Combustion and Thermal Decomposition of GAP

O.P. KOROBENICHEV\*, L.V. KUIBIDA, E.N. VOLKOV, and A.G. SHMAKOV

*Institute of Chemical Kinetics and Combustion, Russian Academy of Science, Novosibirsk 630090, Russia*

Glycidyl azide polymer (GAP) is an active energetic binder in rocket propellants. The main objective of this research was to study the decomposition and combustion chemistry of thoroughly characterized GAP samples to develop a model for the combustion of GAP and propellants based on GAP. The combustion characteristics (burning rates, temperature profiles) and kinetic parameters (order of reaction, activation energy, pre-exponential factor of rate constants) for the thermal decomposition of GAP together with the composition of the products of both the combustion and decomposition of uncrosslinked GAP (with a molecular weight of 350 or 2000) and cured GAP were studied. The flame and thermal decomposition of GAP, as well as the composition of the products were studied using molecular-beam mass-spectrometry (MBMS). The final temperature of a flame of GAP was measured as 1000 to 1100 K. About half of the mass of the combustion products involves large fragments of a polymer without its azide groups. For this reason the mass spectrum obtained on direct MBMS sampling of a flame burning GAP could not be completely interpreted. However, ~47% of the mass of the combustion products was found to be the volatile gases  $N_2$ ,  $H_2$ ,  $CO$ ,  $CO_2$ ,  $CH_4$ ,  $C_2H_4$ ,  $C_2H_6$ ,  $NH_3$ ,  $H_2O$ , acetonitrile, acrylonitrile, and furane, as obtained by mass-spectrometry using freezing/thawing in a liquid nitrogen trap.

The thermal decomposition of thin films of GAP at 1 bar was done in a flow reactor with Ar flowing through it. A tungsten plate was used as a sample heater; its temperature was controlled using a chromel-copel (copel is an alloy of 56.5% Cu, 43.0% Ni and 0.5% Mn) or Pt-PtRh (10%) thermocouples. The thermal decomposition of GAP was studied at a high heating rate over a wide temperature range in three ways: (1) the heating rate was changed from the maximal to the minimal one in the course of decomposition (400–100 K/s); (2) at the linear heating rate (50–400 K/s); (3) fast heating (~400 K/s) to the given temperature and subsequently maintained isothermal. Three stages of thermal decomposition were found. The first stage (yield of nitrogen is ~15%) is a first order reaction. The second stage (yield of  $N_2$  is ~25%) is an autocatalytic one; the third stage is first order and is a weakly exothermic one, with a yield of nitrogen of ~60%. Kinetic parameters (activation energy and pre-exponential factor of rate constants) were found for each stage. The results for both the combustion and thermal decomposition of GAP were compared with literature data and it was concluded that the results strongly depend on the conditions of the experiment and on the source of the GAP. © 2002 by The Combustion Institute

## INTRODUCTION

Azide polymers incorporate one or several  $N_3$  groups per monomer. Their study is of great interest as they can be used as active binders in rocket propellants. The availability of the  $N_3$ -group in a monomer releases additional heat on combustion, giving a higher final combustion temperature and specific impulse. The energy released by an  $N_3$ -group decomposing to  $N_2$  is ~378 kJ/mol [1]. Glycidyl azide polymer (GAP) has the formula:  $OH(-CH_2-CH(CH_2-N_3)-O)_nH$ . Uncured GAP with  $n = 20$  is a viscous yellow liquid under normal conditions. Its density is  $\rho = 1.3 \text{ g/cm}^3$ , adiabatic flame temperature is  $T_f = 1465 \text{ K}$  at  $p = 50 \text{ bar}$  [1]. Cured GAP includes 84.8 wt% of uncured GAP, 12.0

wt% of hexamethylene diisocyanate (HMDI) and 3.2 wt% of trimethylpropane (TMP). Cured GAP has the formula  $C_{3.3}H_{5.6}O_{1.12}N_{2.63}$ , with a density of  $1.27 \text{ g/cm}^3$  and an adiabatic flame temperature of 1365 K at 50 bar [1].

Previous work on GAP as a propellant ingredient can be divided into two groups. The first group is devoted to the study of the combustion of GAP [1, 2], and the second to its thermal decomposition [1, 3–10]. Kubota et al. [1] have measured the burning rate of cured GAP in an atmosphere of nitrogen. The burning rate was found to increase monotonically with pressure from 2.2 mm/s at 4.5 bar to 11 mm/s at 80 bar at the initial temperature  $T_0 = 293 \text{ K}$ . The initial temperature rise of 50 K results in a 1.7-fold rise in burning rate. The calculated mole fractions of the products from the combustion of GAP for equilibrium at 50 bar are:  $0.2234 N_2 + 0.2847 C$

\*Corresponding author. E-mail: korobein@ns.kinetics.nsc.ru

(soot) + 0.1395 CO + 0.0013 CO<sub>2</sub> + 0.0215 CH<sub>4</sub> + 0.3219 H<sub>2</sub> + 0.0071 H<sub>2</sub>O for uncured GAP at 1465 K and 0.1902 N<sub>2</sub> + 0.2983 C (soot) + 0.1393 CO + 0.0035 CO<sub>2</sub> + 0.0368 CH<sub>4</sub> + 0.3152 H<sub>2</sub> + 0.0159 H<sub>2</sub>O for cured GAP at 1365 K.

The flame structure of cured GAP has also been studied [1] using a thin (5 μm) Pt-Rh thermocouple at 4 to 8 bar. Three zones were found in the burning wave. The first zone corresponds to the solid phase heating up by heat conduction, the second one involves reactions in the condensed phase, and the third has reactions in the gaseous phase. The temperature at the burning surface was found [1] to be 700 K. The second zone was established to be the key one in heat release, while heat flow from the gaseous zone to the condensed one can be neglected. Experiments on the thermal decomposition of GAP using differential thermal analysis (DTA) and thermogravimetric analysis (TG) have shown that the decomposition of GAP involves two stages. The first one at 475 to 537 K is exothermic, resulting in a 42% loss of the sample's weight, corresponding to a release of 68% of the nitrogen in the sample. The next stage (T > 537 K) is not exothermic and proceeds more slowly than the first one. Spectroscopic analysis has demonstrated [1] that the -N<sub>3</sub> polymer groups decompose in the first stage to produce N<sub>2</sub> and H<sub>2</sub> with an activation energy of 181.8 kJ/mol. Hori and Kimura [2] considered the combustion of cured GAP as a two-stage process:



First, the azide groups are decomposed in the condensed phase to produce N<sub>2</sub> with a large heat release. Small fragments are formed at this stage. Then oxidation with oxygen atoms in the polymer base yields final products. Farber et al. [3] were the first to use mass-spectrometry in the study of the thermal decomposition of GAP. They found that the GAP is thermally stable at temperatures below 390 K, when the N<sub>3</sub>-group decomposes evolving molecular nitrogen. At temperatures above 440 K a weak peak of ~1 to 2% of that of N<sub>2</sub> indicates HCN as a product of secondary decomposition. Another experimental study [5] of the thermal decomposition of uncured GAP (M<sub>w</sub> = 2000–5000) has used

isothermal thermogravimetry (ITGA and TGA) and IR Fourier spectroscopy (SMATCH-FTIR). ITGA demonstrated that the thermal decomposition of GAP at 453 to 478 K was first order up to a conversion of 0.4. The following kinetic parameters were found: E<sub>a</sub> = 165.5 kJ/mol and pre-exponential factor A = 1.26 × 10<sup>14</sup> s<sup>-1</sup>. From 453 to 493 K TGA with a linear heating rate of 1 K/s showed that E<sub>a</sub> = 165.5 kJ/mol and A = 6.3 × 10<sup>13</sup> s<sup>-1</sup>. The thermal decomposition of thin films of uncured GAP (20–70 μm) were studied by SMATCH-FTIR spectroscopy at a heating rate of 150 K/s, indicating that E<sub>a</sub> = 177.7 kJ/mol and A = 1.0 × 10<sup>19</sup> s<sup>-1</sup> at 515 to 533 K range. It is noteworthy that the thickness of a GAP film is of great importance at the given experimental conditions (at the heating rate of 100–200 K/s). A sample can be significantly hotter than the heater if the GAP film has a large thickness or poor heat transfer. This might result in a discrepancy in the reported kinetic parameters.

The decomposition products of uncured GAP (M<sub>w</sub> ~700) were studied by Arisawa and Brill [6] at 2 bar in argon using T-jump/IR Fourier spectroscopy for thin film samples. There are three types of uncured GAP, which differ in the number of terminal OH-groups: mono-ol, di-ol, tri-ol. The heating rate was as high as 800 K/s. The film thickness varied from 5 to 43 μm. A sample was quickly heated to a given temperature and held at this temperature for 20 s. IR-spectra of the decomposition products were recorded within 3 mm from the sample's surface with a time resolution of 0.1 s. Thus, all three types of GAP were studied from 543 to 593 K. The following products were observed: HCN, NH<sub>3</sub>, CO, CH<sub>2</sub>O, CH<sub>2</sub>CO, H<sub>2</sub>O, CH<sub>4</sub>, C<sub>2</sub>H<sub>4</sub> and GAP oligomers. However, CH<sub>3</sub>CHO and C<sub>2</sub>H<sub>2</sub> were not found. Of course, IR spectroscopy does not detect N<sub>2</sub> and H<sub>2</sub>. A strong dependence of the composition of the decomposition products on the number of OH-groups was revealed.

Haas et al. [7] have studied the laser-supported decomposition (dT/dt ~ 10<sup>7</sup> K/s) of GAP using IR spectroscopy. Nitrogen was analyzed by GC and mass-spectrometry. The main gaseous products found were N<sub>2</sub>, CO, C<sub>2</sub>H<sub>4</sub>, HCN, and possibly H<sub>2</sub>. Here CH<sub>2</sub>O and NH<sub>3</sub> were not detected, but small amounts of acetaldehyde, ethane, propane, propylene and CO<sub>2</sub>

were found. A powder comprising 37 wt% of the initial sample, whose elemental composition was roughly described as  $C_9H_{13}N_3O_2$ , was found in the chamber after decomposition. This powder appeared only at low pressure and small heat fluxes of laser irradiation. If the laser energy pulse was above 150 mJ and helium was present at a pressure above 65 mbar, a thin yellow film was found on the chamber walls instead of the powder. At 400 mbar the amount of HCN was more than an order of magnitude less than in a vacuum. The other gases were not drastically changed by the presence of helium. Addition of  $O_2$  instead of helium produced a similar effect, except for a small amount of NO appearing in the products.

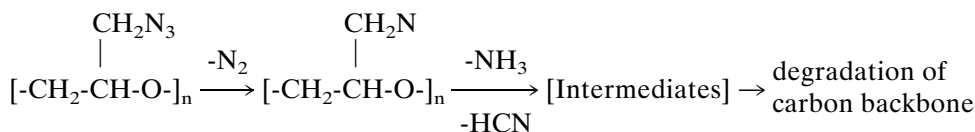
Tang et al. [8] have studied the products from laser-supported decomposition of GAP at 1 bar in argon. The strand surface was heated using a laser flux of 50 to 200 W/cm<sup>2</sup>. The products of decomposition were sampled with a quartz microprobe and transferred to a triple-quadrupole mass spectrometer for analysis from 14 to 150 amu. The signal for masses above 74 amu was below the background level. The products from the composition of GAP had mole fractions as follows: 0.36  $N_2$  + 0.16 HCN + 0.10  $NH_3$  + 0.11 CO + 0.11  $H_2CO$  + 0.09  $CH_3CHO$  + 0.01  $H_2O$  + 0.01  $CH_4$  + 0.01  $C_2H_4$  + 0.09 imines.

The chemical and ballistic properties of GAP and propellants based on GAP have been re-

viewed [9]. In general, the products of the thermal decomposition of GAP are nitrogen, methane, ethane, ethylene, water,  $CO_2$ , propane, benzene, pyrrole, furane, pyridine, HCN, acetaldehyde, ethylene oxide, acetonitrile, formamide, acetone, acetamide, propylene oxide, butadiene, etc. The activation energy of the decomposition is  $E_a = 176.4$  kJ/mol.

Recently Trubert et al. [10] have applied linear pyrolysis using the heated plate method at 940 K and  $10^{-5}$  bar to measure the gaseous products from the decomposition of cured GAP. The procedure of freezing the products in a liquid nitrogen trap (as presented [11] earlier) gave products as: 0.58  $N_2$  + 0.085 CO + 0.064  $NH_3$  + 0.038 HCN + 0.035  $H_2$  + 0.025  $CO_2$  + 0.011  $CH_4$  + 0.007  $H_2O$  + 0.011  $C_2H_2$  + 0.007  $C_2H_4$  + 0.034  $C_2H_6$  + 0.009  $C_3H_4$  + 0.006  $C_3H_6$  + 0.016  $C_3H_8$  + 0.018  $C_4H_8O$  + 0.011  $C_5H_8O$  + 0.005  $C_5H_{10}O$  + 0.052  $NH_2COONH_4$  + 0.014  $NH_2COOC_2H_5$ . The absence of formaldehyde was obvious. Besides there was found a yellowish solid residue (poorly volatile compounds) in the vessel comprising 57 wt% of the initial sample, elemental analysis of which gave  $C_{1.65}H_{1.65}O_{0.40}N_{0.25}$ .

The decomposition of GAP at 1 bar in Ar has been studied [12] at the heating rate of 2 to 5 K/min and led to the following mechanism:



The rate of the decomposition has three maxima at temperatures of  $\sim 498$ , 608, and 698 K. The sample lost 36% of its mass at the first stage and 37% more in the two subsequent stages. The condensed residue comprised  $\sim 27\%$  of the initial mass of GAP. It has been found [13] from IR-spectra that above 493 K the rate of release of  $CO_2$  is first order with an activation energy of  $\sim 168$  kJ/mol, which is close to the energy of disruption of a N-N<sub>2</sub> bond in azide group [13]. The kinetics of thermal decomposition of GAP has been studied [14, 15] by others.

Preliminary results of our investigations on the kinetics of thermal decomposition of GAP

have been presented [11]. This paper is devoted to a further study of its thermal decomposition using molecular beam mass-spectrometry (MBMS) in isothermal and non-isothermal conditions at both slow and fast heating, the latter being close to the heating rate in a combustion wave in GAP. Also attempts were made to find an approximate composition of the products. It is likely that the products depend on the structure of GAP and also the experimental conditions. There are no data on the composition of the products from combusting GAP. The results should be useful when developing combustion models for GAP; these always require the com-

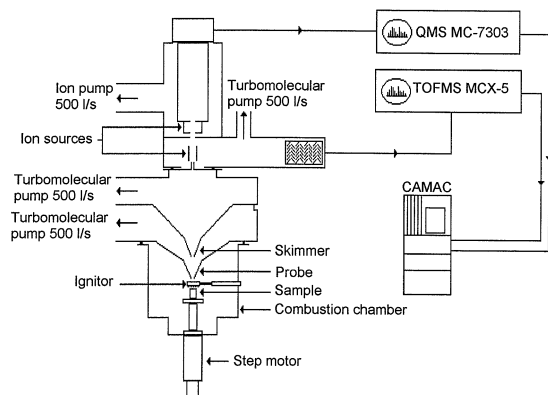


Fig. 1. MBMS setup for sampling the flames of condensed systems.

position of products from the destruction of the binder as a boundary condition. As GAP is capable of self-sustaining combustion, it is necessary to know the composition of the combustion products when GAP is used as a monopropellant.

## EXPERIMENTAL

### Properties of Compounds

Uncured liquid GAP which was synthesized at St. Petersburg Technological University has the following characteristics:

Molecular structure:



Molecular weight: 1976

Density: 1275 kg/m<sup>3</sup>

Heat of formation: 611 kJ/kg

Content of -(OH) groups: 2.58 wt%

Chemical formula: C<sub>50</sub>H<sub>99</sub>O<sub>17</sub>N<sub>44</sub>

Cured GAP was also used in some experiments for comparison with uncured GAP. GAP cured by the standard procedure with HMDI was synthesized in St. Petersburg Technological University.

### Setup for Investigation of Combustion of GAP

The molecular beam sampling system for investigating flames of condensed systems is schematized in Fig. 1. Its main feature is that it works with two types of spectrometer: time-of-flight mass-spectrometer (TOFMS) and quadrupole

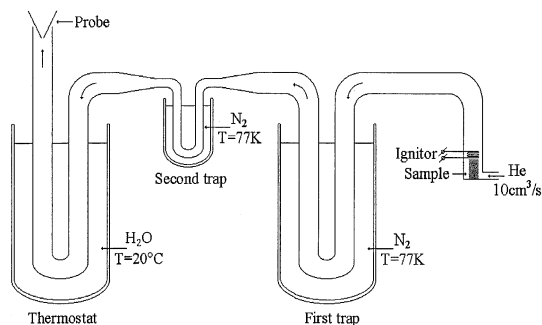


Fig. 2. The setup for additional separation of combustion products in a liquid nitrogen trap in a helium flow.

mass-spectrometer (QMS). The TOFMS (MCX-5) is very fast as required to study rapidly burning energetic materials. Six selected mass-spectral peaks could be measured every 20 ms with a 100-fold accumulation and averaging with a sweep frequency of 10 kHz (10000 spectra/s) using specially designed CAMAC electronic units. The quadrupole mass-spectrometer (MC-7303) is much more sensitive and sweeps a spectrum from mass 2 to mass 130 in 1 s. Its operating mass range is 2 to 520 amu. The QMS data acquisition system was assembled from standard CAMAC units: Analog-Digital Converter, Digital-Analog Converter and Timer. A specially developed code controlled the data acquisition system. Mass-spectra of the combusting products from GAP were measured by direct flame sampling using either TOFMS or QMS mass-spectrometer with a quartz probe with a 100 μs orifice for 1 bar and 20 μm for 5 bar.

Mass-spectra obtained by direct sampling are difficult to interpret. To provide additional separation of the combustion products in the mass-spectrometric analysis, the products were frozen in a liquid nitrogen trap and subsequently slowly defrosted in a flow of helium. Lengellé et al. [16] were the first to apply this method to propellants. The setup is presented in Fig. 2. The experiment was performed at 1 bar by placing 0.2 ml of GAP in a glass vial [3 mm i.d. (internal diameter)] at whose face an ignition spiral was set. The helium flow was ~10 cm<sup>3</sup>/s. After all the temperatures were set, the QMS data acquisition system was started, and the GAP was ignited. During the combustion of GAP and subsequent transfer of the combustion products,

the mass-spectra of the products not frozen out (e.g., N<sub>2</sub>, CO, CH<sub>4</sub>, and H<sub>2</sub>) were measured. Then without stopping the helium flow the first trap was slowly defrosted, its contents being refrozen in the second one. When the first trap was completely defrosted, mass-spectral measurements were started again and liquid nitrogen was removed from the second trap. The defrosting procedure took ~10 min at natural heating in air. The trap was immersed in a vessel of warm water at the end of the process.

Application of the quadrupole mass-spectrometer improved the sensitivity of the molecular-beam sampling system; in fact, the ratio of signal/background increased by an order of magnitude for mass numbers from 2 to 130. Also we succeeded in improving the separation of the combustion products owing to the smaller internal volume of the second trap. A trap of smaller volume provided more uniform heating and less smearing along the flow on thawing. Better separation of gases with close boiling points was achieved. In this trap all the gases volatile up to 370 K and frozen at liquid nitrogen temperature were gradually refrozen in the flow of helium.

Calibration experiments were performed on the same setup as that used for measuring the combustion products. A tube made of silicon rubber was inserted in the feed-line of the sample to enable a gas sample to be injected by a syringe. A 5-mL syringe was used to feed gases and a 20- $\mu$ L syringe to feed liquids. The time course of mass-spectral peak changes was measured after supplying the gas, and the calibration coefficient of the gas was found with respect to helium:  $K_i(\text{He}) = (S_i \times V_{\text{He}})/(S_{\text{He}} \times V_i)$ , where  $V_i$  is the volume of the introduced gas;  $S_i$  is the area under the curve of the changes in the most intensive peak of the calibrated gas;  $V_{\text{He}}$  is the volume of helium in a given time interval, and  $S_{\text{He}}$  is the area under the curve of the temporal changes of the peak of mass 4, corresponding to the above volume. The volume usually introduced was enough to provide a nearly constant peak of mass 4. Calibrations were made for N<sub>2</sub>, CO<sub>2</sub>, H<sub>2</sub>, NH<sub>3</sub>, HCN, H<sub>2</sub>CO, and H<sub>2</sub>O. To calibrate H<sub>2</sub>O, a drop of water (20  $\mu$ L) was heated to a temperature of about 330 K in a flow of helium. Calibration coefficients for

other gases were estimated using data in the database [18].

When the flux of introduced gas was high, complete displacement of helium took place. In this case a strong dependency of  $K_i$  on gas concentration was observed. Actually, such a displacement was observed in the experiment only when non-frozen gases were detected; that is why we applied an additional 10-fold dilution with helium when measuring non-frozen gases. This provided correct use of calibration results. To obtain summary mass-spectra of volatile products, experiments were conducted without freezing the combustion products from uncured GAP on the same setup.

### Temperature Profiles

To measure the temperature profile with cured GAP, a strand of GAP (8  $\times$  8  $\times$  10 mm) was cut from the side of the base to a depth of ~5 mm. In this section a  $\Pi$ -shaped thermocouple (30  $\mu$ m; WRe(5%)-WRe(20%)) was inserted parallel to the burning surface. The strand was compressed with a metal envelope to provide better thermal contact between the thermocouple and polymer. In both cases ignition was performed with an electrically heated spiral.

### Setup for Investigating Thermal Decomposition of GAP

The experiments on thermal decomposition at 1 bar were performed on a setup and with a molecular-beam probe system of sampling and time-of-flight mass-spectrometer [19]. GAP was thermally decomposed in a flow reactor in Ar of ~4 cm<sup>3</sup>/s. The flow reactor is shown in Fig. 3; it was a quartz tube (i.d. of 10 mm) with two narrow gaps (3 mm long), through which passed a tungsten plate (width: 3 mm; thickness: 0.2 mm; length: 25 mm for cured GAP, but width: 0.7 mm; thickness: 0.1 mm; length: 25 mm for uncured GAP) used to heat the sample. There was no thermal contact between this plate and the quartz tube. The plate was heated by an electric current. The plate's temperature was controlled using a thermocouple of either chromel-copel (a ribbon 20–30  $\mu$ m thick) or Pt-PtRh (10%) (a ribbon 5–7  $\mu$ m thick), welded to the tungsten plate. A quartz probe (orifice

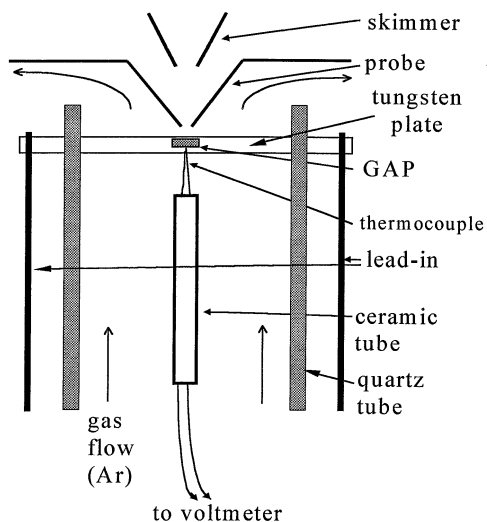


Fig. 3. Flow reactor for GAP thermal decomposition at pressure 1 bar.

diam. 0.08 mm) was used for sampling. The distance from the plate to the probe was ~1 to 5 mm. It is noteworthy that the intensity of a mass's peak is proportional to the rate of evolution of the decomposition products under these experimental conditions. A sample of uncured GAP was applied to the plate from a solution of it in acetone (1:10). The volume of the applied solution was ~0.1 to 0.2 mm<sup>3</sup>, corresponding to ~0.02 mg of GAP. The sample was dried for 2 to 3 min in Ar flowing at 5 cm<sup>3</sup>/s. Evaluations confirmed that the mass-spectrometric method used is a differential one in such conditions, because ~0.01 cm<sup>3</sup> of N<sub>2</sub> evolved from 0.02 mg of GAP within the reaction time of ~1 s. This means that the ratio of the flow-rates of decomposition products to that of Ar is ~1/100 to 1/500. The time for the products to reach the probe was ~0.02 s. When

studying cured GAP, polymer samples with width of 3 mm, length of 3 mm and thickness of 0.03–0.05 mm were used. Such a sample was made as follows: GAP was frozen in liquid nitrogen and then a thin chip was cut with a cooled scalpel. The sample of 0.7 to 0.5 mg was cramped between two tungsten plates heated by an electric current during the experiment.

## EXPERIMENTAL RESULTS

### Burning Rates

The burning rate of uncured GAP in Ar at 1 bar (see Table 1) turned out to be very high (18.3 mm/s). Direct video-recording the combustion of liquid GAP in a glass beaker (i.d. 8 mm, length 20 mm) showed that the burning liquid's surface was not flat, but had the shape of a funnel of irregular form, whose depth exceeded the beaker's diameter. Designating this combustion mode as "turbulent," the dependence of the burning rate of GAP on pressure in argon was investigated. The burning rate was measured using thermocouples to indicate a flame front. Table 1 shows that at low pressures (<4 bar), the burning rate grows linearly with pressure, but afterwards it falls abruptly as the combustion mode is changed. The uncertainty in the burning rate at 1 to 4 bar is 1 mm/s. At ~5 bar there is a transient regime and the burning rate of uncured GAP at this pressure differs from experiment to experiment. The temperature of the final products, as measured by a W-Re thermocouple at 1 bar, was found to be 1080 ± 40 K. Table 1 contains the measured burning rates for uncured and cured GAP in argon (initially at room temperature, T<sub>0</sub>, if not

TABLE 1

The Burning Rate of Uncured and Cured GAP in Argon

Uncured GAP (quartz vial, diam. 8 mm)							
P, bar	1	2.1	3.2	4	5.0	5.2	10
U, mm/s	18.3 ± 1	23.5 ± 1	29.3 ± 1	28.5 ± 1	5.5	12.8	5.0
Cured GAP (strand in square cross section 5.5 mm, length 8 mm)							
P, bar	1 (T <sub>0</sub> = 120°C)		6	10	20		
U, mm/s	10 ± 1		3.7	6.3	7.3 ± 0.2		

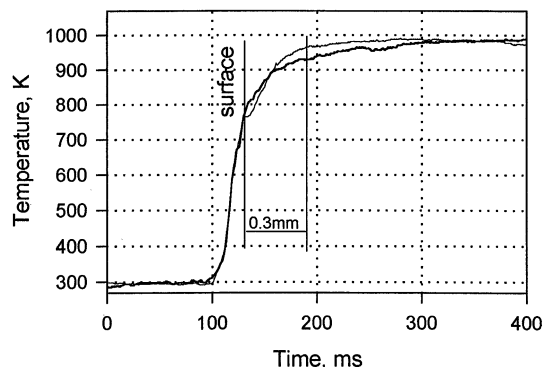


Fig. 4. Temperature profiles of combustion wave of cured GAP at 20 bar of argon.

otherwise stated). Cured GAP was found to be ignited at 370 K at 1 bar in nitrogen or argon, but its steady combustion was achieved only at 390 K. At the initial temperature of the room a strand was completely burnt out at 5 bar and above.

### Temperature Profiles

Figure 4 presents the measured temperature profiles in the combustion wave from cured GAP in argon at 20 bar. The temperature of the final products ranged up to 980 K. A skeleton of soot remained after burning and constituted  $\sim 2$  wt% of the original sample. At 760 and 810 K sharp bends were observed on the temperature plot; they are associated with the protrusion of the thermocouple into the gas-phase and interpreted as the surface temperature being  $785 \pm 25$  K. These data agree and supplement those of Kubota et al. [1].

### Composition of the Products from the Combustion of Uncured GAP

The detection procedure for non-condensable gases did not undergo any essential changes from those used previously [11], except that the sample was also diluted immediately in front of the probe. This was conducted to rule out any effect of separation by mass in a molecular beam. Figure 5 demonstrates the evolution of peaks for the non-frozen gases  $N_2$ , CO,  $H_2$ , and  $CH_4$  at the outlet of the thermostat after burning GAP strand in He  $\sim 10$  cm<sup>3</sup>/s. The mole

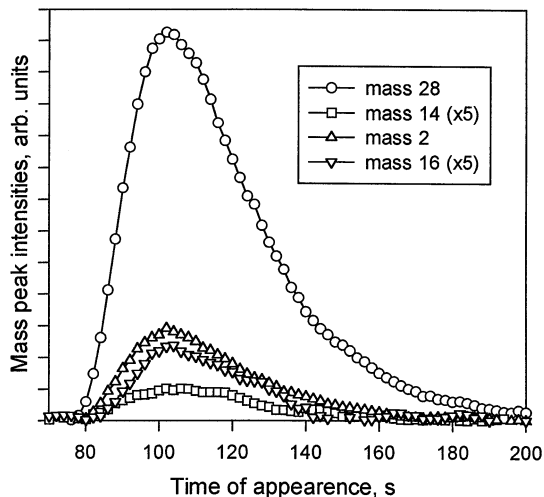


Fig. 5. The time course of mass peak intensities of non-frozen gases  $N_2$ , CO,  $H_2$ , and  $CH_4$  after burning of a GAP strand in flowing helium.

fractions of these non-condensable gases were:  $0.73 N_2 + 0.21 CO + 0.05 H_2 + 0.01 CH_4$ . Separation of  $N_2$  and CO with the same mass of 28 was by the peak at mass 14, to which only  $N_2$  contributes.

The appearance of condensable combustion products from uncured GAP during thawing is shown in Fig. 6. Data analysis was started by identifying the groups of mass spectral peaks appearing simultaneously in mass spectra. Eleven such groups were obtained. Then for each group the species were identified by the ratio of mass peak intensities, taking into account the b.p. of applicants. A mass spectral library [17] was used to identify the species responsible for groups of peaks. The identification of gases found before [11] was confirmed with good accuracy:  $H_2$ ,  $N_2$ , CO,  $CO_2$ ,  $CH_4$ ,  $C_2H_4$ ,  $C_2H_6$ ,  $C_3H_6$ ,  $NH_3$ , and  $H_2O$ . Besides, acetonitrile (masses 40, 41), acrylonitrile (masses 52, 53), furane (masses 68, 39) were detected.

The analysis of each group of peaks is given below. The first group of peaks corresponds to ethylene (b.p. = 169 K) and ethane (b.p. = 184 K). The second group corresponds to  $CO_2$ , whose sublimation temperature is 194 K. The third group corresponds to propylene (b.p. = 226 K). Several compounds (masses 50, 51, 54) with close mass-spectra and an overall formula  $C_4H_6$  form the next group. They possibly are

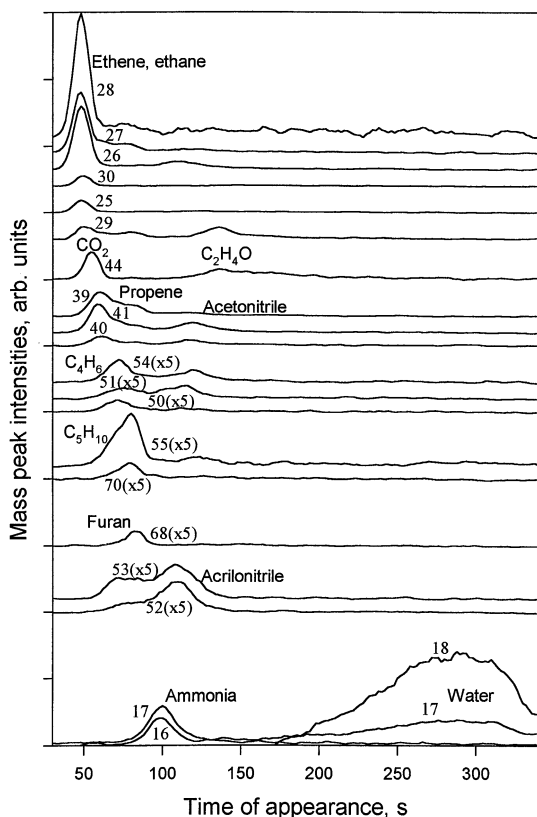


Fig. 6. The time dependence of some mass peak intensities during the defreezing of GAP combustion products.

1,3-butadiene, butene-1, or butene-2. Thus, the compounds responsible for this group escaped identification. For the same reason a group of peaks with masses of 55 and 70 has not been identified. This could be pentene-2 or 1-butene-2-methyl with an overall formula  $C_5H_{10}$ . The sixth group was identified as furane (b.p. = 304 K). The seventh group is ammonia (b.p. = 240 K). The eighth group was identified as acrylonitrile (b.p. = 350 K). The ninth group was acetonitrile (b.p. = 355 K). The next group at masses 44 and 29 was not strictly identified. It may be either acetaldehyde, or ethylene oxide with an overall formula  $C_2H_4O$ ; they have very similar mass-spectra and boiling points. Finally, the eleventh group corresponds to water (b.p. = 373 K).

Some disruption in the correlation between the retention time of defreezing gases with their boiling point can be explained by a high solubility in water of ammonia, which is found in large

amounts. The failure to find any traces of HCN in the combustion products of GAP is noteworthy. It is formed in the decomposition of GAP but must react very near to the burning surface. Of course, compounds identified as products of the combustion of uncured GAP using freezing-thawing were used for interpreting the mass-spectra without freezing the combustion products.

### The Decomposition of Uncured GAP

Experiments on the thermal decomposition of uncured GAP were performed in three ways: (1) the heating rate was changed from the maximal to the minimal one during decomposition (400–100 K/s); (2) using the linear heating rate (50–400 K/s); (3) fast heating ( $\sim 400$  K/s) to the given temperature, which subsequently was maintained constant, giving isothermal conditions. To check the temperature measurements, the temperature in a GAP lamina during thermal decomposition was measured. For this purpose a GAP sample was applied to the heating plate from its solution in acetone (1:10), then a rolled (flat) Pt-PtRh (10%) thermocouple 5 to 7  $\mu\text{m}$  thick was placed in position and more GAP was applied. The absence of thermal contact between the thermocouple and heating plate was checked before and after thermal decomposition by measuring the electrical resistance between them. The experiments were performed both in isothermal and non-isothermal conditions. Measurements showed that the temperatures in the GAP lamina and at the plate's surface differed by less than 4 K. Theoretical evaluations based on the experimentally measured reaction rate and heat of reaction (624 kJ/mol) [1] demonstrate that the maximal temperature difference between a thermocouple and sample is  $\sim 3$  K for a GAP lamina 20  $\mu\text{m}$  thick, without considering heat transfer in the gas-phase. In fact, the GAP lamina was  $\sim 1/10$ th the thickness. That is why the temperature difference between the sample and thermocouple (and, consequently, the error in temperature determination) was less than 0.3 K.

In the thermal decomposition of GAP with a nonlinear heating rate, three maxima for the intensity of the peak with  $m/e$  28 were found, this intensity being proportional to the rate of

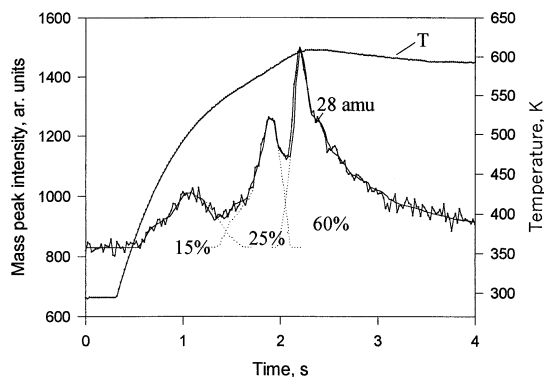


Fig. 7. Thermal decomposition of uncured GAP with a nonlinear heating rate.

evolution of  $N_2+CO$ . These maxima are shown in Fig. 7; they correspond to three successive stages in the thermal decomposition of GAP. Pfeil et al. [12] and Trubert et al. [10] also reported that GAP decomposes in three steps. The first stage was not connected with any impurity in GAP. Thus, the absence of solvent (acetone) in the sample was confirmed by the absence of a peak with  $m/e = 58$  in the mass-spectra of the products. When GAP was decomposed isothermally at a relatively low temperature of 555 K, there was only one maximum for the peak with  $m/e = 28$ , as shown in Fig. 8a. This means that only the first decomposition stage is revealed. Analysis established that this stage follows first order behavior. Two stages (see Fig. 8b) were observed at the higher isothermal temperature of 565 K. However, the rate of the second stage is described by an autocatalytic law. At higher temperatures the two maxima are likely to interfere with each other, so it is difficult to distinguish between them. That is why in Fig. 8c only one maximum was observed at 579 K. Based on these observations it was concluded that several stages take place, which can be studied in isolation of each other under certain conditions. It was found indirectly that the thermocouple was indicating that the second stage is strongly exothermic.

The thermal decomposition of cured GAP was studied in less detail than uncured GAP, because of the experimental difficulties in making thin layers of cured GAP. The heating rate was 2 to 5 K/s. Only one decomposition stage was observed under these conditions. The de-

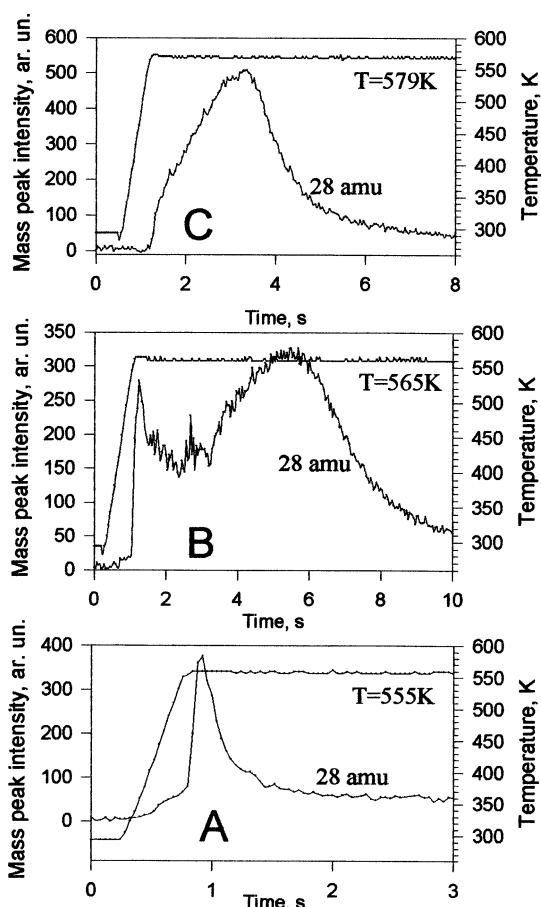


Fig. 8. Thermal decomposition of uncured GAP under isothermal conditions.

composition was accompanied by heat release and sometimes resulted in a so-called “burst” with an abrupt release of both heat and the products from decomposing GAP.

### The Products from Decomposing GAP

The thermal decomposition of GAP yields different, but known species. Interpretation of the mass-spectra obtained presents certain difficulties related both to the complexity of the composition of these products and to the insufficient mass-spectrometric database available. However, an attempt was made to find the composition of the products, using the available measurements supplemented with data from the literature. The composition of the products from uncured GAP was derived from mass-

TABLE 2

Kinetic Parameters for the Non-Isothermal Decomposition of Cured GAP (from Fig. 7)

Stage	1	2
$E_i$ , kJ/mol	$68 \pm 8$	$124 \pm 11$
$A_i$ , $s^{-1}$	$2.5 \times 10^5$	$1 \times 10^{12}$

spectra for isothermal decomposition in the second stage.

**Kinetics of Thermal Decomposition**

We failed to find the separate contributions from  $N_2$  and CO in the peak with  $m/e = 28$ . However, as literature data testify [6, 9, 10],  $N_2$  makes the main contribution to the peak at mass 28. The rate of decomposition of GAP is proportional to the intensity of this peak at  $m/e = 28$ . Three successive stages were found in the experiments, as mentioned above. For isothermal conditions at 555 K the first stage proceeds much faster than the second one, which is not observed at this temperature. The analysis showed that the rate of conversion for the first stage is first order, but the second follows an autocatalytical law. The third stage proceeds much more slowly than the second and is hardly revealed at 555 to 579 K.

The results presented in Fig. 9 were obtained for the thermal decomposition of uncured GAP with a linear heating rate. It is apparent that the

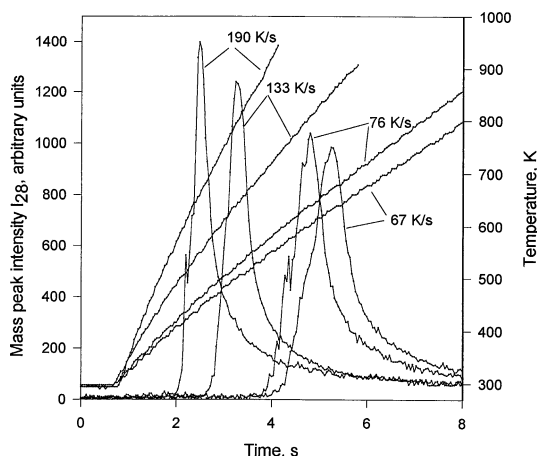


Fig. 9. Thermal decomposition of uncured GAP at different linear heating rates.

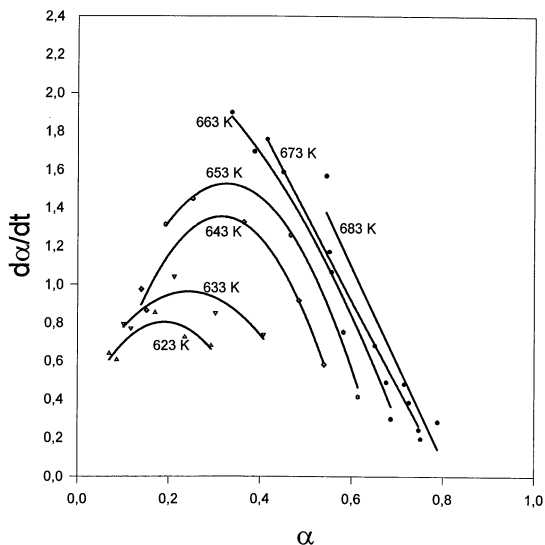


Fig. 10. Dependency of the rate of decomposition of uncured GAP on conversion,  $\alpha$ , at constant temperature.

profiles for the peak at  $m/e = 28$  show one maximum. This information allowed the dependence of the reaction rate on conversion,  $\alpha$ , for isothermal conditions to be found using the method described elsewhere [20]. The results are plotted in Fig. 10 and indicate that the second stage is autocatalytical. Thus at 625 to 653 K the maximum rate of decomposition was found between  $\alpha = 0.2$  and 0.3. Figure 11

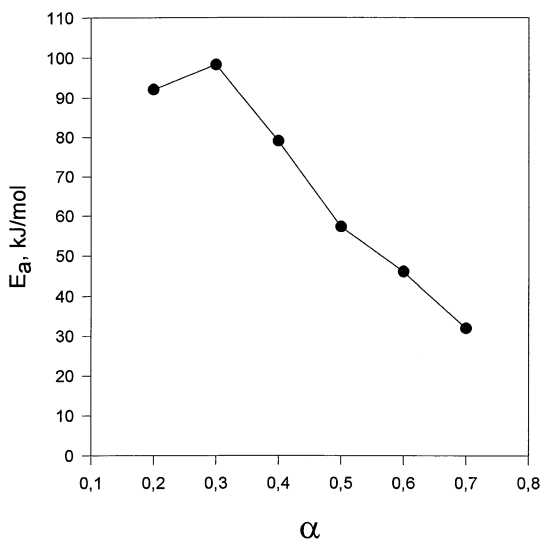
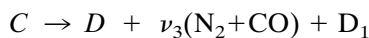
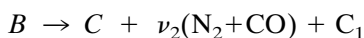
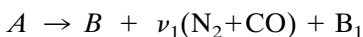


Fig. 11. Dependency of the activation energy,  $E_a$ , for the decomposition of uncured GAP on the conversion  $\alpha$ .

presents the dependence of the activation energy for the decomposition of GAP on the conversion  $\alpha$  for  $\alpha = 0.2$  to  $0.7$ , derived using the data in Fig. 10. The complicated dependence in Fig. 11 supports a multistage mechanism for the decomposition of GAP. The activation energy at  $\alpha = 0.3$  is  $E_a = 97 \pm 10$  kJ/mol and at  $\alpha = 0.7$  is  $E_a \sim 30$  kJ/mol. It is noteworthy that processing the same experimental measurements assuming first order behavior [5] gives an activation energy for the second stage about twice as large, that is,  $\sim 180$  kJ/mol.

The decomposition with a nonlinear heating rate is shown in Fig. 7. It reveals three stages during one experiment. To find the kinetic parameters these results were also processed. They suggest that the maxima correspond to the following three successive stages:



Here B and C are intermediate condensed products, D is the condensed final reaction product, but  $B_1$ ,  $C_1$ ,  $D_1$  are gaseous reaction products. The ratio of the areas under the curves for each of the three processes is proportional to the ratios of the molar yields of  $N_2 + CO$  in the total process:  $\nu_1:\nu_2:\nu_3 = 15:25:60$ . The kinetic parameters were found, suggesting that the 1<sup>st</sup> stage is a first order reaction; the second one is autocatalytical (the reaction rate is  $W_2 = k_2\alpha_2(1 - \alpha_2)$ , where  $\alpha_2$  is conversion in the second stage). An Arrhenius dependence for the rate constants of the first and the second stages is checked in Fig. 12 and Table 2. The third stage occurs nearly isothermally ( $\Delta T \leq 12$  K). It was a first order reaction with a rate constant at  $T \sim 600$  K of  $k_3 = 2.2$  s<sup>-1</sup>.

## DISCUSSION

### Combustion of GAP

The experimental measurements indicated the products of combustion to be those shown in Table 3. The total mass of these products comprised 0.47 g per gram of GAP. Besides, a dark yellow film (involatile below 370 K) remained in

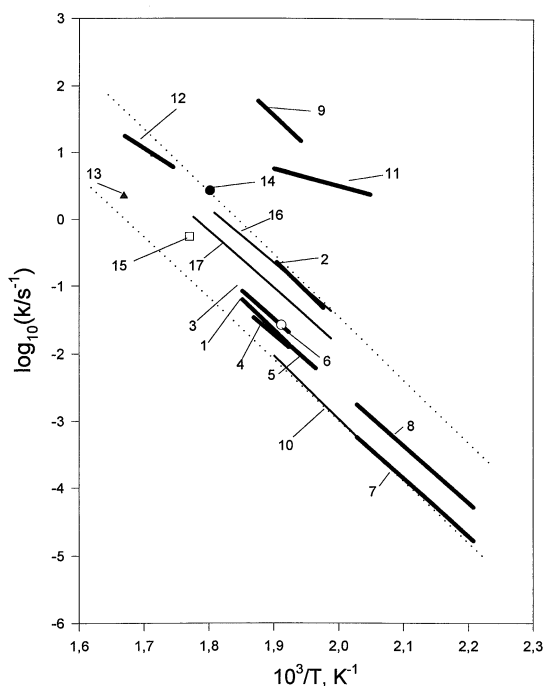


Fig. 12. Arrhenius plots of the rate constant for the thermal decomposition of GAP.

the trap after thawing. A similar residue was found on the vessel's walls after thermally decomposing GAP at 400 mbar [7] and in a vacuum [10]. The condensate's mass comprised, respectively, 37 wt% [7] and 57 wt% [10] of the original sample of GAP. In our case the mass of condensate was found by direct weighing and comprised not less than 0.46 g per g of GAP. Haas et al. [7] have suggested the elementary composition of the condensed product to be  $C_9H_{13}N_3O_2$ , but Trubert et al. [10] quote  $C_9H_{7.44}N_{2.28}O_{3.56}$ . Using the composition of the gaseous products obtained in this work, a material balance indicates the condensate to be:  $C_9H_{13.8}N_{2.8}O_{1.4}$ , that is, very similar to that from Haas et al. [7]. This means that the overall reaction is  $[-OCH(CH_2N_3)CH_2-] \rightarrow 1.08 N_2 + 0.32 CO + 0.26 H_2O + 0.07 H_2 + 0.035 NH_3 + 0.016 C_2H_4 + 0.014 CH_4 + 0.014 CO_2 + 0.005 C_3H_6 + 0.004 C_3H_3N + 0.003 C_2H_6 + 0.003 C_2H_3N + 0.001 C_4H_4O + \text{condensate} + \text{unidentified products}$ .

The error for  $N_2$  does not exceed  $\pm 20\%$ . It is connected with separating the peak at 28 (into  $N_2$  and CO) using fragmentary peak at mass 14.

TABLE 3  
The Composition of Uncured GAP Combustion Products

	N <sub>2</sub>	CO	CO <sub>2</sub>	CH <sub>4</sub>	C <sub>2</sub> H <sub>4</sub>	C <sub>2</sub> H <sub>6</sub>	C <sub>3</sub> H <sub>6</sub>
mg/g GAP	306	89.6	6.2	2.3	4.5	0.9	2.2
accuracy	± 20%	± 20%	± 10%	± 30%	± 30%	± 30%	± 30%
	H <sub>2</sub>	NH <sub>3</sub>	H <sub>2</sub> O	Acrylonitrile	Acetonitrile	Furane	
mg/g GAP	1.4	6.0	47.9	1.9	1.1	0.7	
accuracy	± 20%	± 10%	± 30%	± 30%	± 30%	± 30%	

That is why within experimental error it is true that one monomer of GAP yields one molecule of N<sub>2</sub>. As no experimental data on the products from the self-sustaining combustion of GAP in an inert atmosphere are available in the literature, the data obtained here may be compared with the results from the thermal decomposition of GAP. This is done in Table 4. As for the literature data in Table 4, N<sub>2</sub> (as well as H<sub>2</sub>) was not measured by Arisawa et al. [6] because of limitations of their FTIR procedure; however estimates of the possible nitrogen-content are given in Table 4. It is clear from Table 4 that our measurements are in good agreement, not only

with those of Tang et al. [9] with respect to [N<sub>2</sub>]/[CO] and also [CH<sub>4</sub>] and [C<sub>2</sub>H<sub>4</sub>], but also with Trubert et al. [10] with respect to almost every species measured except for NH<sub>3</sub>, H<sub>2</sub>O, and HCN. The main advantage of our technique over previous ones is its ability to detect hydrogen and measure its concentration. The absence of hydrogen, except in the studies of Trubert et al. [10], is probably attributable to the use of IR-spectrometers, gas chromatography without a special column or a mass-spectrometer [3, 9] with a mass sweep starting at only 12 or 14 amu. Only Trubert et al. [10] have measured [H<sub>2</sub>], and their data are in good

TABLE 4  
Product Composition (mole fractions) from the Combustion and Thermal Decomposition of GAP

	N <sub>2</sub>	CO	NH <sub>3</sub>	CO <sub>2</sub>	H <sub>2</sub> O	HCN	CH <sub>4</sub>	C <sub>2</sub> H <sub>4</sub>	C <sub>2</sub> H <sub>6</sub>	C <sub>3</sub> H <sub>6</sub>	H <sub>2</sub>	CH <sub>3</sub> CN
Our data <sup>a</sup>	0.59	0.18	0.02	0.01	0.14	0	0.01	0.01	0.002	0.003	0.04	0.002
Our data <sup>b</sup>	0.50	0.25	0.02	0.02	0.13	0	0.001			0.01	—	0.004
Our data <sup>c</sup>		0.56*	0.05	0.14	0.09	0.05						
Chen [5]	0.36	0.24	0.06			0.17	0.03	0.03				
Arisawa [6]	0.25	0	0.19		0	0.11	0.13	0.15				
Haas [7]	0.40	0.27		trace		0.005	0.06	0.10	trace	trace	?	
Haas [7]	0.40	0.27		trace		0.09	0.06	0.09	trace	trace	?	
Tang [9]	0.36	0.11	0.10		0.01	0.16	0.01	0.01				
Trubert [10]	0.58	0.08	0.10	0.016	0.01	0.04	0.02	0.01	0.03	0.004	0.05	
	C <sub>2</sub> H <sub>3</sub> CH	C <sub>4</sub> H <sub>4</sub> O	CH <sub>2</sub> O	CH <sub>3</sub> CHO	Imines	C <sub>2</sub> H <sub>2</sub>	H <sub>2</sub> CCO	Conditions				
Our data <sup>a</sup>	0.002	<0.001						U, 1bar				
Our data <sup>b</sup>	0.008	0.003	0.01					U, 1bar				
Our data <sup>c</sup>			0.11					U, 565K				
Chen [5]			0.09				0.01	U, 533K, 1bar				
Arisawa [6]			0.11					U, 593K, 2bar				
Haas [7]					trace		0.03	C, 400 mbar				
Haas [7]					trace		0.04	C, vacuum				
Tang [9]			0.11	0.09	0.09			C, 1bar				
Trubert [10]			0		0.02	0.01		C, 940 K, vacuum				

\* —N<sub>2</sub> + CO; <sup>a</sup> —combustion (with freezing); <sup>b</sup> —combustion (without freezing); <sup>c</sup> —thermal decomposition (the second stage), C—cured, U—Uncured.

agreement with ours. As for ethane, propylene, acetonitrile, acrylonitrile, and furane observed by us, we believe that the sensitivity at the disposal of others was not high enough, since the amount of these compounds was rather small.

We reconstructed the mass-spectrum of the volatile combustion products of GAP by summing the mass-spectra of non-condensed combustion products and also the mass-spectra of the combustion products obtained when freezing-thawing combustion products. We have compared this mass-spectrum, normalized to the intensity of mass peak 28, with the mass-spectra of the combustion products from GAP obtained by direct sampling (i.e., the mass-spectrum of all products including volatile products and products which condensed as a film). The intensities of mass peaks in such a "reconstructed" mass-spectrum (with the exception of the peaks at 17 and 18 amu, attributable to water) were one tenth smaller than the same intensities in the second mass-spectrum. It was assumed that  $N_2$  and CO give the peak at 28 amu. Next the "reconstructed" mass-spectrum was subtracted from the mass-spectrum obtained by direct sampling. It is obvious that the resulting spectra corresponded to that of the condensed products. The intensities of almost all the peaks (except for the peaks at 17, 18, and 28 amu) changed by only  $\sim 10\%$  after subtraction. Consequently, only condensed products (the yellow film) contribute to these peaks in the mass-spectrum obtained by direct sampling. Thus, the mass-spectrum of the combustion products of GAP obtained by direct sampling (except for masses 17, 18, and 28) corresponds to unidentified products with high molecular weights condensed as a yellow film (or residue) on the reactor's walls.

As mentioned above, we did not succeed in finding any evidence from any mass-spectral peaks appearing in the thawing process for the presence of HCN. This is not connected with any inability of our method to detect HCN. The calibration experiments using HCN provided evidence for the absence of HCN in the products from burning uncured GAP. The introduction of a small quantity of HCN (of  $\sim 1 \text{ cm}^3$ , giving  $\sim 5\%$  of the volume of the frozen combustion products) to the frozen combustion

products resulted in the detection of HCN during thawing. The time of appearance of the peaks for HCN during thawing corresponded with the boiling point of HCN. Special calibration experiments were made for both HCN and  $NH_3$ . A mixture of these species was entered in a flow of He and frozen in the trap. These experiments provided evidence that HCN and  $NH_3$  were being detected and determined in these mixtures. HCN is formed during the decomposition of GAP (we detected it), but during the combustion of GAP it must react very near the burning surface. This is probably why we did not detect it in the products from burning GAP.

In comparison with others we have detected large amounts of water. This result was repeated in many experiments. The amount of water was calculated using the calibration coefficient measured by us. Tang and Litzinger [8] used experimental conditions closer to ours for the combustion of GAP than other studies. They detected less water, but instead of water they found large amounts of other oxygen-containing species ( $CH_2O$  and  $CH_3CHO$ ), not formed in our work. They investigated cured GAP, and its laser-supported decomposition, but not uncured GAP and its combustion. Therefore, discrepancies in the composition of the products are attributable to the different experimental conditions and the type of GAP used.

### Thermal Decomposition of GAP

The composition of the products from decomposing GAP was calculated based both on our and literature calibration data on mass-spectra. Consequently, the composition found is an approximate one. However, it is of interest to compare it with those in the literature. Our measurements in Table 4 are in satisfactory agreement with the literature data on  $NH_3$  [5, 9, 10], HCN [7, 10], and  $CH_2O$  [5, 6, 9]. There is a large diversity between our measurements and previous measurements [9, 10] on  $H_2O$ , [10] on  $CO_2$  and [6] on most species. Possibly, this is a result of different samples of GAP, conditions of experiment and experimental procedures.

A mass-spectrum of the non-identified products was obtained by subtracting mass-spectra of

TABLE 5

Mass-Spectrum of the Products of Non-Identified Products of GAP Thermal Decomposition, Normalized for the Intensity of Peak 43 amu

amu	15	17	28	29	30	31	39	43
$I_i/I_{43}, \%$	18	7	22	16	16	33	14	100

the identified products (HCN, CH<sub>2</sub>O, CO<sub>2</sub>, H<sub>2</sub>O, NH<sub>3</sub>, N<sub>2</sub>, and CO) from the mass-spectrum of the decomposition products. It was normalized for the intensity of the peak at 43 amu and is given in Table 5. According to the mass-spectrometric database this mass-spectrum can be attributed to species such as CH<sub>3</sub>C(O)(CN), C<sub>2</sub>H<sub>5</sub>OH, CH<sub>3</sub>OH, CH<sub>3</sub>CHCN, etc. Figure 12 and Table 6 give the Arrhenius dependencies of the rate constants from different authors and our work. The rate constants for the first stage obtained at high heating rates  $\sim 60$  to 100 K/s (our data and data from [5]: curves 11 and 9) are 2 to 3 orders of magnitude larger than the results obtained at low heating rates of  $\sim 0.1$  K/s by different methods (curves 1–8, 10) and our previous results for relatively thick films (30–50  $\mu\text{m}$ ) of cured and uncured GAP [11] (curves 16 and 17) at heating rates of 2 to 5 K/s. The rate constants for the second and third stages with non-linear

heating rates (curve 12, point 13) and for the first and second stages under isothermal conditions (points 14 and 15) are also grouped around the dependency corresponding to many literature data for experiments at low heating rates. This is the area between the two dotted lines in Fig. 12. The scatter in this area results from different samples of GAP, methods of investigation and methods of data processing. It should be noted that these two experimental sets differ also in the weight of the samples and, consequently, in the thickness of samples studied. Thin samples of  $\sim 1 \mu\text{m}$  were used for high heating rates, and in the first experimental set the samples were likely to be 2 to 3 orders of magnitude thicker. The reason for these differences in kinetic data can be associated with the dependency of the reaction rate on the sample's thickness, and possibly on its heating rate. To the best of our knowledge the dependency of decomposition rate on a sample's thickness has not been studied yet.

## CONCLUSIONS

The final products from burning uncured GAP at normal pressures were: N<sub>2</sub>, H<sub>2</sub>, CO, CO<sub>2</sub>, CH<sub>4</sub>, C<sub>2</sub>H<sub>4</sub>, C<sub>2</sub>H<sub>6</sub>, NH<sub>3</sub>, H<sub>2</sub>O, acetonitrile, ac-

TABLE 6

Arrhenius Parameters for GAP Thermal Decomposition

Curve in Fig. 12	$E_a, \text{kJ/mol}$	$A, \text{s}^{-1}$	T, K	Method	Cond <sup>a</sup>	Order	Stage	Ref.
1	178.1	$7 \times 10^{15}$	520–540	DSC	U	0.8	?	[14] <sup>b</sup>
2	182.7	$2.2 \times 10^{16}$	506–525	DSC	U	0.8	?	[14] <sup>b</sup>
3	163.8	$4 \times 10^{14}$	520–540	DSC	U	0.8	?	[14] <sup>b</sup>
4	152.9	$2 \times 10^{13}$	520–535	DSC	C	0.8	?	[14] <sup>b</sup>
5	159.6	$1 \times 10^{14}$	509–519	FRMS	?	?	?	[14] <sup>b</sup>
6	174.3	$4.5 \times 10^{15}$	523	DSC	?	1	?	[15] <sup>b</sup>
7	165.5	$1.26 \times 10^{14}$	453–478	ITGA	U	1	?	[5]
8	165.5	$6.3 \times 10^{13}$	453–493	TGA	U	1	?	[5]
9	177.7	$1 \times 10^{19}$	515–533	SMATCH	U	1	?	[5]
10	180	$7.5 \times 10^{15}$	483–526	TGA	C	1	1	[10]
11	68.0	$2.5 \times 10^5$	488–550	TOFMS	U	1	1	our data
12	124	$1.0 \times 10^{12}$	570–600	TOFMS	U	autocatalytic	2	our data
13		$k = 2.2, \text{s}^{-1}$	$\sim 600$	TOFMS	U	1	3	our data
14		$k = 2.7, \text{s}^{-1}$	555	TOFMS	U	1	1	our data
15		$k = 0.6, \text{s}^{-1}$	565	TOFMS	U	autocatalytic	2	our data
16	157.9	$7.29 \times 10^{14}$	503–553	TOFMS	U	1	1	[11]
17	165.1	$1.56 \times 10^{15}$	503–563	TOFMS	C	1	1	[11]

<sup>a</sup> C—cured, U—uncured; <sup>b</sup> —cited from [6].

rylonitrile, and furane. A condensable residue constituted 46% by weight of the products, in good agreement with the literature on the thermal decomposition of GAP. This residue is the main contributor to the mass spectrum obtained by direct MBMS sampling of the combustion products from GAP.

The kinetics of thermal decomposition of thin films of GAP was studied at a high heating rate of 100 to 200 K/s, which is close to the conditions in a burning wave in GAP, as well as in isothermal conditions. Three stages for the process were found. The first (nitrogen yield ~ 15%) is a first order reaction. The second stage (nitrogen yield ~ 25%) is autocatalytic, but the third is a first order and weakly exothermic, with a nitrogen yield of ~60%. Kinetic parameters were found for each stage. The data obtained are compared with available literature data; it is concluded that the results strongly depend on the conditions of an experiment.

*This work was supported by EOARD under Contract F61708 to 97-WO195. The authors thank Thomas Brill for fruitful discussion of the paper.*

## REFERENCES

1. Kubota, N., and Sonobe, T., *Propellants, Explosives, Pyrotechnics* 13:172 (1988).
2. Hori, K., and Kimura, M., *Propellants, Explosives, Pyrotechnics* 21:160 (1996).
3. Farber, M., Harris, S. P., and Srivastava, R. D., *Combust. Flame* 55:203 (1984).
4. Oyumi, Y., and Brill, T. B., *Combust. Flame* 65:127 (1986).
5. Chen, J. K., and Brill, T. B., *Combust. Flame* 87:157 (1991).
6. Arisawa, H., and Brill, T. B., *Combust. Flame* 112:533 (1998).
7. Haas, Y., Eliahu, Y. B., and Welner, S., *Combust. Flame* 96:212 (1994).
8. Tang, C. J., and Litzinger, T. A., *Combust. Flame* 117:244 (1999).
9. Nazare, A. N., Asthana, S. N., and Singh, H., *J. Energetic Materials* 10:43 (1992).
10. Trubert, J.-F., Duterque, J., and Lengellé, G., *Thirtieth International Annual: Conference of ICT*, Fraunhofer Institut Chemische Technologie, Karlsruhe, 1999, pp. 23.1–23.17.
11. Korobeinichev, O. P., Kuibida, L. V., Shmakov, A. G., and Paletsky, A. A., AIAA-paper-99-0596.
12. Pfeil, A., and Löbbbecke, S., *Propellants, Explosives, Pyrotechnics* 22:137–142 (1997).
13. Wentrup, C., *Reactive Molecules*. Wiley, New York, 1984, p. 162.
14. Goshgarian, B. B., AFRPL –TR-82–040, Air Force Rocket Propulsion Laboratory, Edwards AFB, CA, June, 1982.
15. Lengellé, G., et al., *Twenty-ninth Joint Propulsion Conference, Monterey, CA, AIAA-93-2413*, 1993.
16. Lengellé, G., Bizot, A., Duterque, J., and Trubert, J.-F., in *Fundamentals of Solid-Propellant Combustion*, Vol. 90 of Progress in Astronautics and Aeronautics, 1984.
17. *NIST/EPA/NIH mass spectral library (NIST 98) and NIST mass spectral search program, Version 1.6*, National Institute of Standards and Technology, USA, 1998.
18. *Mass spectral data*, Am. Petroleum Institute Research Project 44, NY, 1952.
19. Korobeinichev, O. P., Kuibida, L. V., Paletsky, A. A., and Shmakov, A. G., *J. Propulsion and Power* 14:991–1000 (1998).
20. Merzhanov, A. G., *Fizika Gorenia i Vzryva* 1:4 (1973) [in Russian].

*Received 28 September 2001; revised 26 November 2001; accepted 2 December 2001*